THE JOURNAL OF BIOLOGICAL CHEMISTRY VOL. 285, NO. 23, pp. 17974–17985, June 4, 2010

Mammalian Numb-interacting Protein 1/Dual Oxidase Maturation Factor 1 Directs Neuronal Fate in Stem Cells*[S]

Received for publication, November 13, 2009, and in revised form, March 8, 2010 Published, JBC Papers in Press, March 16, 2010, DOI 10.1074/jbc.M109.084616

Karen A. M. Kennedy[‡1,2], **Elena A. Ostrakhovitch**[‡1,3], **Shelley D. E. Sandiford**[‡], **Thamara Dayarathna**[‡], **Xiaojun Xie**[‡], **Elaine Y. L. Waese**[§**4], **Wing Y. Chang**[¶], **Qingping Feng**[‖], **Ilona S. Skerjanc**[‡**], **William L. Stanford**[§¶5], **and Shawn S. C. Li**[‡6]

From the [‡]*Department of Biochemistry, Siebens-Drake Medical Research Institute, Schulich School of Medicine and Dentistry and the* [‖]*Department of Physiology and Pharmacology, the University of Western Ontario, London, Ontario N6A 5C1, Canada, the* [§]*Department of Chemical Engineering and Applied Chemistry and the* [¶]*Institute of Biomaterials and Biomedical Engineering, University of Toronto, Ontario M5S 3G9, Canada, and the* **Departments of Biochemistry, Microbiology, and Immunology, University of Ottawa, Ottawa, Ontario K1H 8M5, Canada*

In this study, we describe a role for the mammalian Numb-interacting protein 1 (Nip1) in regulation of neuronal differentiation in stem cells. The expression of Nip1 was detected in the developing mouse brain, embryonic stem cells, primary neuronal stem cells, and retinoic acid-treated P19 embryonal carcinoma cells. The highest expression of Nip1 was observed in undifferentiated neuronal stem cells and was associated with Duox1-mediated reactive oxygen species ROS production. Ectopic *nip1* expression in P19 embryonal carcinoma cells induced neuronal differentiation, and this phenotype was also linked to elevated ROS production. The neuronal differentiation in *nip1*-overexpressing P19 cells was achieved in a retinoic acid-independent manner and was corroborated by an increase in the expression of the neuronal basic helix-loop-helix transcription factors and neural-lineage cell markers. Furthermore, depletion of *nip1* by short hairpin RNA led to a decrease in the expression of neuronal basic helix-loop-helix transcription factors and ROS. However, inhibition of ROS production in *nip1*-overexpressing P19 cells restricted but did not extinguish neuronal differentiation. Microarray and mass spectrometry analysis identified intermediate filaments as the principal cytoskeletal elements affected by up-regulation of *nip1*. We show here the first evidence for a functional interaction between Nip1 and a component of the nuclear lamina, lamin A/C. associated with a neuronal-specific phenotype. Taken together, our data reveal an important role for Nip1 in the guidance of neuronal differentiation through ROS generation and modulation of intermediate filaments and implicate Nip1 as a novel intrinsic regulator of neuronal cell fate.

Factors that modulate neuronal differentiation are not fully understood. Their elucidation, particularly in stem cells, is desirable because of potential use in the development of therapies for treatment of neurodegenerative and neurodevelopmental disorders. The *neurogenins* and *mash* are examples of early-acting proneural genes that initiate neurogenesis, whereas *math* and *neuroD* family members act later to promote neuronal differentiation (1–5). Other factors such as Sox and Hes inhibit expression or function of these proneural genes to maintain some cells in their progenitor state (6). Expression of proneural and neuronal inhibitory genes is down-regulated during terminal differentiation, which is marked by appearance of pan-neuronal markers such as doublecortin, neuronal cell-specific βIII-tubulin, and neurofilament (7–9).

Embryonic neural stem (NS)[7] cells and adult neural stem cells reside in specific tissue niches such as hippocampal subgranular and subventricular zones. These cells are capable of generating new cells for fetal development and homeostasis in adult brain. NS cells possess a limited developmental potential and are considered neuronal-restricted progenitors (10). Pluripotent embryonic stem (ES) or embryonal carcinoma (EC) cells can be induced to differentiate into cell types from all three germ layers. Aggregation of P19 EC cells in the presence of micromolar concentrations of retinoic acid (RA) induces their differentiation into the neuroectodermal derivatives. The differentiation of P19 cells provides a useful model system for identification and characterization of factors that regulate neuronal differentiation and development (11).

Dual oxidase 1 and 2 (Duox 1 and 2) are members of the NADPH oxidase superfamily of enzymes expressed mainly in thyroid and epithelial cells of various origins (12). Duox proteins are required for generation of H_2O_2 during thyroid hormone biosynthesis (13–15). We previously identified the Numb-interacting protein (Nip) in a screen for proteins that bind to the cell fate determinant Numb (16); however, the role of Nip has not as yet been studied for a function related to cell

* This work was supported by grants from the Canadian Institute of Health Research (to I. S. S., W. L. S., and S. S. C. L.) and by Genome Canada through the Ontario Genomic Institute (to S. S. C. L.).

[S] The on-line version of this article (available at http://www.jbc.org) contains supplemental Methods, Tables 1 and 2, and Figs. S1–S5.

[1] Both authors contributed equally to this work.

[2] Supported by Ontario graduate scholarships, University of Western Ontario.

[3] Present address: Dept. of Chemistry, University of Western Ontario, London, Ontario N6A 5C1, Canada.

[4] Supported by Ontario graduate scholarships, University of Toronto.

[5] Holds a Canada Research Chair in Stem Cell Bioengineering and Functional Genomics.

[6] Holds a Canada Research Chair in Functional Genomics and Cellular Proteomics. To whom correspondence should be addressed: 1400 Western Rd., SDRI, Schulich School of Medicine and Dentistry, UWO, London, ON N6A 5C1, Canada. Tel.: 519-850-2910; Fax: 519-661-3175; E-mail: sli@uwo.ca.

[7] The abbreviations used are: NS, neural stem; ES, embryonic stem; EC, embryonal carcinoma; RA, retinoic acid; Duox, Dual oxidase; Nip, Numb-interacting protein; RT, reverse transcription; qRT, quantitative reverse transcription; DCX, doublecortin; MnTBAP, manganese(III) *meso*-tetrakis(4-benzoic acid) porphyrin; DCF, dichlorofluorescein; ROS, reactive oxygen species; shRNA, short hairpin RNA; scrRNA, scrambled shRNA; MS, mass spectrometry; PGK, phosphoglycerate kinase.

fate determination. The mammalian homologue Nip1 was subsequently re-identified as Duoxa1, a Duox1 maturation factor (17).

Neuronal morphogenesis and establishment of correct neuronal functioning requires cytoskeleton remodeling through coordinated orchestration of cytoskeletal components (18). The intermediate filaments of neurons undergo dynamic changes and actively participate in controlling neurogenesis. The member of type V intermediate filaments, lamins, are involved in nuclear organization by forming structures intercalated between chromatin and the inner nuclear membrane, DNA replication, and transcription, which are related to cell differentiation (19–21). The expression of A-type lamins (lamins A/C) is associated with differentiated tissue and was shown to be present in mature and nearly mature neurons of rat brain (22–26).

The present study investigates the role of mammalian Nip1/Duoxa1 in neuronal differentiation. Nip1 is expressed in the developing brain, and we found that it was differentially regulated during differentiation of NS, ES, and P19 EC cells. The highest level of Nip1 expression was observed in NS cells and coincided with elevated Duox-mediated hydrogen peroxide release, in contrast with decreased Nip1 and hydrogen peroxide levels in terminally differentiated neurons. Ectopic expression of Nip1 in P19 cells resulted in elevation of intracellular reactive oxygen species (ROS), induction of neuron-specific gene expression, and ultimately, neuronal differentiation. Loss of function analysis indicated a role for Nip1-mediated ROS generation in neurogenesis. Microarray and mass spectrometry analyses demonstrated that Nip1 may affect cytoskeletal components resulting in expression of intermediate filament and actin anchoring proteins. Ectopic expression of Nip1 led to up-regulation of lamin A/C, resulting in acquisition of the specific phenotype of neuronal cells.

EXPERIMENTAL PROCEDURES

Plasmids and Expression Constructs—A 1.6-kb cDNA fragment containing the complete coding sequence of mouse *nip1* (BC019755) tagged with a c-Myc epitope was inserted into the phosphoglycerate kinase (PGK) vector via the SmaI/Xho1 restriction sites. The empty PGK vector was used as a control. Constructs for PGK-puro and B17 were as previously described (27). The nip1 short hairpin RNA (shRNA) expression constructs consisted of pairs of short hairpin DNA sequences complementary to regions of the nip1 gene (see supplemental Table 1) inserted into the mU6Pro vector (a gift from Dave Turner, University of Michigan, Ann Arbor, MI) after digestion with Bbs/1 and Xho1 as previously described (28). A scrambled sequence (previously described in Ref. 29) was inserted into the mU6Pro vector to serve as a negative control. The green fluorescent protein expression construct was based on pEGFP-C3 (Invitrogen).

Cell Culture and Isolation of Stable Cell Lines—P19 EC cells (American Type Culture Collection) were cultured as described previously (30). Neuronal differentiation was induced with 1 μM RA in α-minimum essential media supplemented with 5% fetal bovine serum (Sigma) and 5% newborn calf serum (Gibco). Myogenic differentiation was induced as described in Ref. 31). P19[*nip1*] stable cell lines were created by transfecting P19 cells with the construct PGK-*nip1* or the empty PGK vector along with the constructs PGK-Puro and B17 using the FuGENE 6 HD transfection kit (Roche Diagnostics) as per the manufacturer's instructions. Cultures were examined for Nip1 expression by immunofluorescence and by end-point reverse transcription (RT)-PCR. Selected Nip1-expressing cells and control cells were grown under puromycin selection until distinct colonies were formed (in ~10 days). Individual colonies were transferred to 24-well plates, grown to confluence, and duplicated. Three independent clonal populations of stable clones, P19[*nip1*]-1, -2, and -9, and two control clones, P19[control]-9 and -10, were used in the experiments described.

To examine the role of Nip1 in P19 cell differentiation, P19[*nip1*] or P19[control] cells were cultured without chemical treatment and examined for differentiation at the desired time points. Differentiation assays were repeated three-six times. For suppression of Nip1 expression, P19 cells were transfected, using FuGENE 6, with the mU6pro vector containing shRNA oligos directed against two different regions of the *nip1* gene. Cells transfected with vectors that contained scrambled shRNA sequences were used as controls. To monitor transfection efficiency, cells were co-transfected with a pEGFP-C3 expression construct. At 24–48 h post-transfection, cells were analyzed for *nip1* mRNA, Nip1 protein, and for intracellular H_2O_2 concentration.

Primary mouse neural progenitor cells were isolated from the periventricular tissue of postnatal day 5 C57BL/6 mouse brain (Charles River Laboratories). Mice were housed and bred in the Health Sciences Animal Care Facility at the University of Western Ontario according to standards of the Canadian Council for Animal Care. All procedures were monitored under a protocol approved by the University of Western Ontario Council on Animal Care. Cells were isolated and then induced to differentiate into neurons marked by βIII tubulin expression (supplemental Fig. S2*B*) on polyornithine-coated dishes as previously described (32).

E14 ES cells were cultured on mouse embryonic fibroblasts with ES cell maintenance medium containing leukemia inhibitory factor (Chemicon). For embryoid body differentiation, 1×10^5 E14 ES cells were seeded into each well of a 6-well low-cluster plate and cultured in embryoid body differentiation medium. Embryoid body differentiation medium was similar to ES cell maintenance medium except for the absence of leukemia inhibitory factor and the use of FBS from Invitrogen. All cultures were maintained at 37 °C under 5% CO_2.

Statistical Analysis—Statistical analysis was performed with Student's *t* test. *p* values of $p < 0.05$ are indicated as *asterisks* and are considered statistically significant.

RESULTS

Nip1 Expression in Embryos and Developing Brain—RT-PCR analysis revealed that *nip1* transcripts were expressed in several different organs of adult mice including brain (Fig. 1*A*). For the first time, we show that *nip1* is expressed in brain tissue. In contrast, *nip2* transcripts were not detectable in brain tissue (Fig. 1*A*). Therefore, we explored a physiological role for the

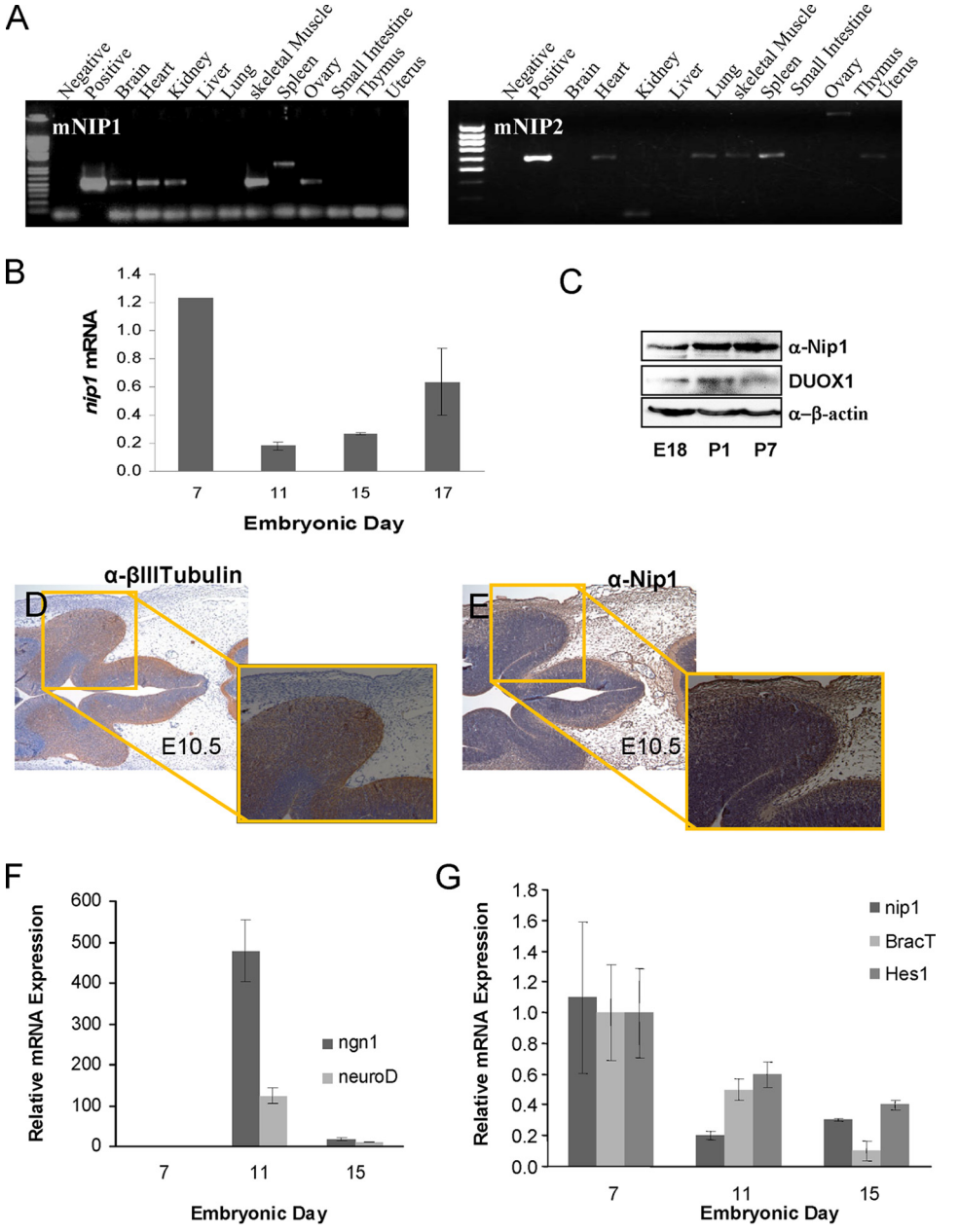

FIGURE 1. **Expression analysis of Nip1 in mouse brain.** *A*, shown is detection of the *nip1* and *nip2* transcripts in mouse (*m*) tissues as determined by RT-PCR. *B*, temporal expression pattern of Nip1 in mouse embryos from embryonic day 7 to embryonic day 17 are shown. The expression levels were based on qRT-PCR data obtained from a pool of embryos for each day. *C*, detection of Nip1 protein in mouse brain is shown. Western blot analysis of total protein extract from brain at embryonic day 18 (*E18*) and postnatal days 1 (*P1*) and 7 (*P7*) is shown. *D* and *E*, immunostaining of coronal sections from E10.5 brains with anti-Nip1 and anti-tubulin III antibodies. The nuclei on the section were stained by hematoxylin. Higher magnifications of the boxed regions are shown in D and E. *F*, temporal expression patterns of *neurogenin1* and *neuroD* in mouse embryos of E7, E11, and E15 are shown. *G*, temporal expression patterns of *nip*, *brachyuryT*, and *hes1* in mouse embryos are shown. The expression levels were based on qRT-PCR data and are shown as -fold changes over their respective levels at E7. An *error bar* represents the S.D. of duplicates from a pool of embryos.

mammalian *nip* homologue in the acquisition of the neuronal fate. First, we determined the temporal expression pattern of Nip1 in developing mouse embryos and brain. Quantitative reverse transcription (qRT)-PCR analysis showed a gradual decrease in *nip1* transcripts from embryonic day 7 to embryonic day 15 with a subsequent increase at day 17 (Fig. 1*B*). A rabbit polyclonal antibody was raised against mouse Nip1. The specificity of this antibody was confirmed by loss of immunoreactivity in Western blot after preincubating cell lysate with the Nip1 peptide antigen (supplemental Fig. S1*A*). Western blot analysis anti-revealed the presence of the Nip1 in fetal and postnatal brain tissue. A pronounced increase in Nip1 expression was observed from embryonic day 18 (E18) to postnatal day 7 (Fig. 1*C*). At E10.5, the immunohistochemical analysis of the coronal sections of brain showed that Nip1 was strongly expressed in several areas of brain. In particular, the expression was detected in the periventricular zone and neuroepithelium. Additionally, Nip1 was expressed in the intermediate zone of the developing layer and in the ganglionic eminences, where neurons migrate to the pial surface. Most importantly, Nip1 was expressed in all areas of cerebral peduncle from which an important neuron population starts its differentiation process. Nip1 staining showed overlapping patterns with that of βIII-tubulin (Figs. 1*D*, supplemental Fig. S1*D*). Hence, these data confirm the presence of Nip1 in neurogenic regions of the developing brain. Because Nip1 has been associated with Numb, which was shown to play a critical role in neurogenesis in *Drosophila* and mouse (35–38), it was important to determine the expression pattern of Numb. We found that the distribution pattern of Numb was distinct from that of Nip1 (supplemental Fig. S2). We next compared the expression of *nip1* mRNA to genes known to be involved in early embryonic development at various time points during mouse embryonic development. Expression of the proneuronal bHLH factors *neurogenin1* or *neuroD* was undetectable at E7 but increased at E11 when cortical neurogenesis was initiated (33) (Fig. 1*F*). In contrast, the expression of *nip1* decreased from E7 to E11. This temporal mRNA expression of *nip1* closely resemble that of the repressive bHLH transcription factor *hes1* (34) and *brachyuryT*, a gene known to pattern the early mesoderm (35) (Fig. 1*G*). The temporal pattern of the *nip*1 expression suggests that it may function in global organization of the early embryo, upstream of the bHLH proneuronal factors.

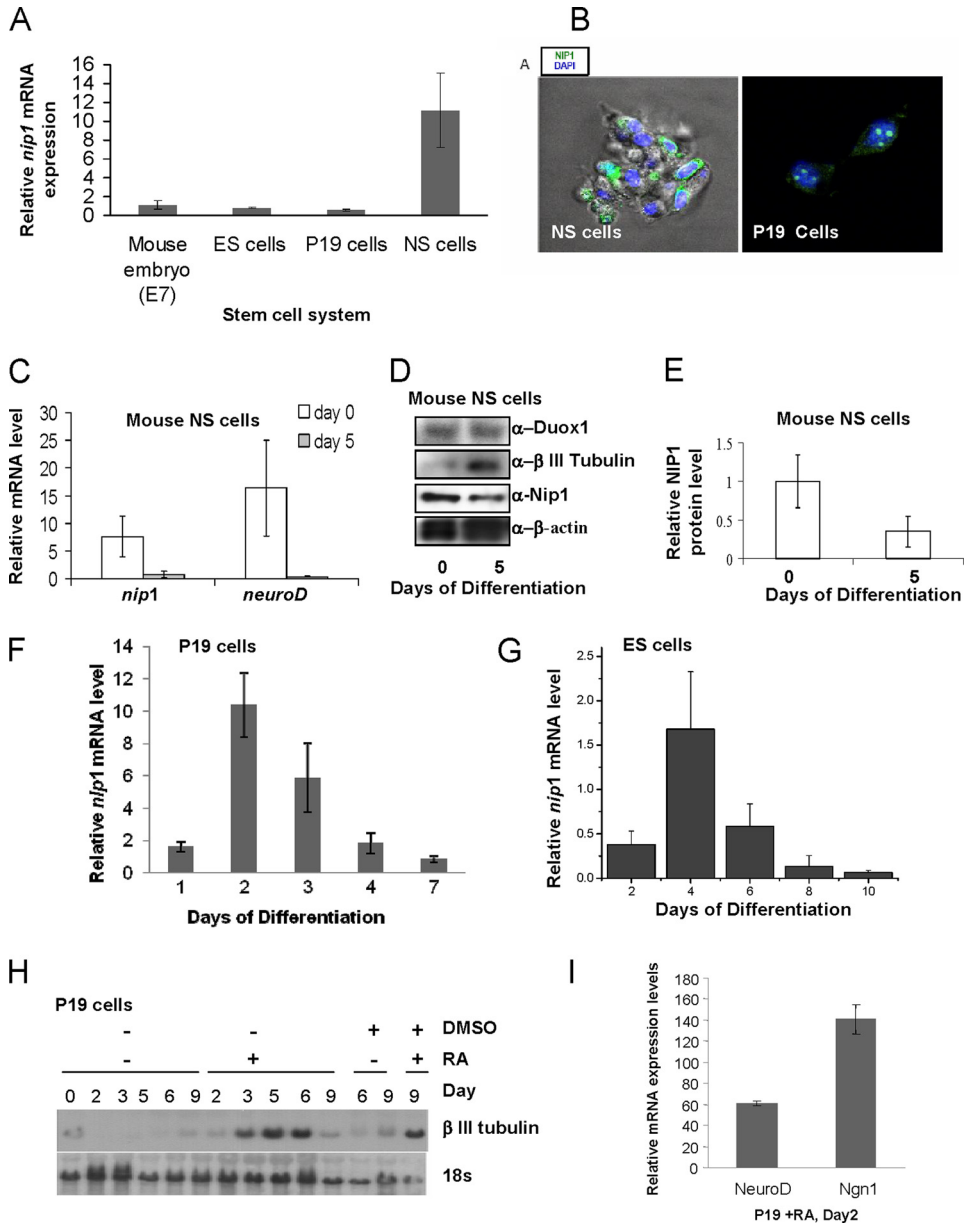

FIGURE 2. **Up-regulation of Nip1 precedes neuronal differentiation in stem cells.** *A*, shown is *nip1* expression in stem cells and mouse embryos as examined by qRT-PCR. The transcript levels of *nip1* were normalized to that of glyceraldehyde-3-phosphate dehydrogenase and then compared with the level of *nip1* mRNA of the mouse embryo at E7. *B*, anti-Nip1 immunofluorescence images of mouse primary NS cells and P19 EC cells are shown. Magnification is 6300×. *C*, the expression of *nip1* and *neuroD* during differentiation of primary neural stem cells was examined by qRT-PCR; $p < 0.05$ (*) and $p < 0.001$ (**)compared with day 0. *D*, Western blot analysis of Nip1, Duox1, and βIII-tubulin in differentiated and undifferentiated primary neural stem cells is shown. *E*, the relative protein level, determined by densitometry of the WB bands, for Nip1 on day 5 of differentiation was compared with that on day 0. The level of Nip1 was normalized to that of actin before the comparison; **, $p < 0.001$ *versus* day 0. An *error bar* represents the S.D. of three independent experiments. *F*, a temporal pattern of *nip*1 expression during RA-induced neuronal differentiation of P19 cells as assessed by qRT-PCR is shown. Expression levels are shown as -fold changes over the level of *nip1* on day 0. An *error bar* represents the S.D. of two independent experiments. *G*, shown is the temporal pattern of *nip1* expression during mouse ES cell differentiation determined by qRT-PCR. PCR was performed in triplicates for three biological replicates. *H*, P19 cells were aggregated in the absence and presence of 1 μM RA to induce neuronal differentiation and with DMSO alone or DMSO with RA to induce myogenic differentiation. Cells were harvested for RNA at the indicated time points. The induction of neurogenesis in RA-treated cultures was confirmed by an up-regulation in the neuronal specific marker βIII-tubulin. *I*, shown is expression of *neurogenin1* and *neuroD* on day 2 of RA-induced neuronal differentiation of P19 cells relative to day 0. An *error bar* represents the S.D. of two independent experiments.

Nip1 Expression in Stem Cells—We examined Nip1 expression in several mammalian stem cell systems during neuronal differentiation. Analysis by qRT-PCR revealed that the *nip1* transcript was enriched in tissue-committed primary neuronal stem cells compared with pluripotent cells isolated from E7 mouse embryos and undifferentiated ES or P19 EC cells (Fig. 2*A*). Examination of the subcellular localization of Nip1 revealed ubiquitous distribution in ES cells (not shown), primary NS cells, and P19 EC cells (Fig. 2*B*, supplemental Figs. S1*B* and S2*B*). These data suggest that Nip1 expression is tightly regulated in stem cells and may be involved in the transition from pluripotent to a more restricted developing state. Because Nip1 was up-regulated in primary NS cells and developing brain tissue, we investigated the role of Nip1 in regulating mammalian stem cell differentiation toward the neuronal lineages.

Up-regulation of Nip1 Expression Precedes Neuronal Differentiation of Stem Cells—Unlike pluripotent P19 EC and mouse ES cells, non-differentiated, tissue-restricted NS cells from mouse periventricular tissue expressed a relatively high basal level of Nip1 (Fig. 2, *A–C*). Under differentiation conditions these cells produce neurons that express βIII-tubulin but not nestin, an intermediate filament protein expressed predominantly in undifferentiated stem cells (Fig. 2*D* and supplemental Fig. S2*B*). PCR analysis showed that the level of *neuroD* mRNA was decreased upon differentiation, indicating that these NS cells underwent neuronal differentiation (Fig. 2*C*). Furthermore, a significant decline in *nip1* mRNA (Fig. 2*C*) and Nip1 protein levels (Fig. 2, *D* and *E*) ($p < 0.05$) was observed as the primary NS cells terminally differentiated.

P19 cells aggregated in the presence of 1 μM RA differentiated into the neuronal lineage as confirmed by the expression of neuronal markers such as neurofilament and βIII-tubulin on day 7 by immunofluorescence and Western blot (supplemental Fig. S3, *A* and *B*). In accordance with our previous data (31), Northern blot analysis showed that βIII-tubulin expression was elevated by RA treatment, whereas there was minimal differentiation in the absence

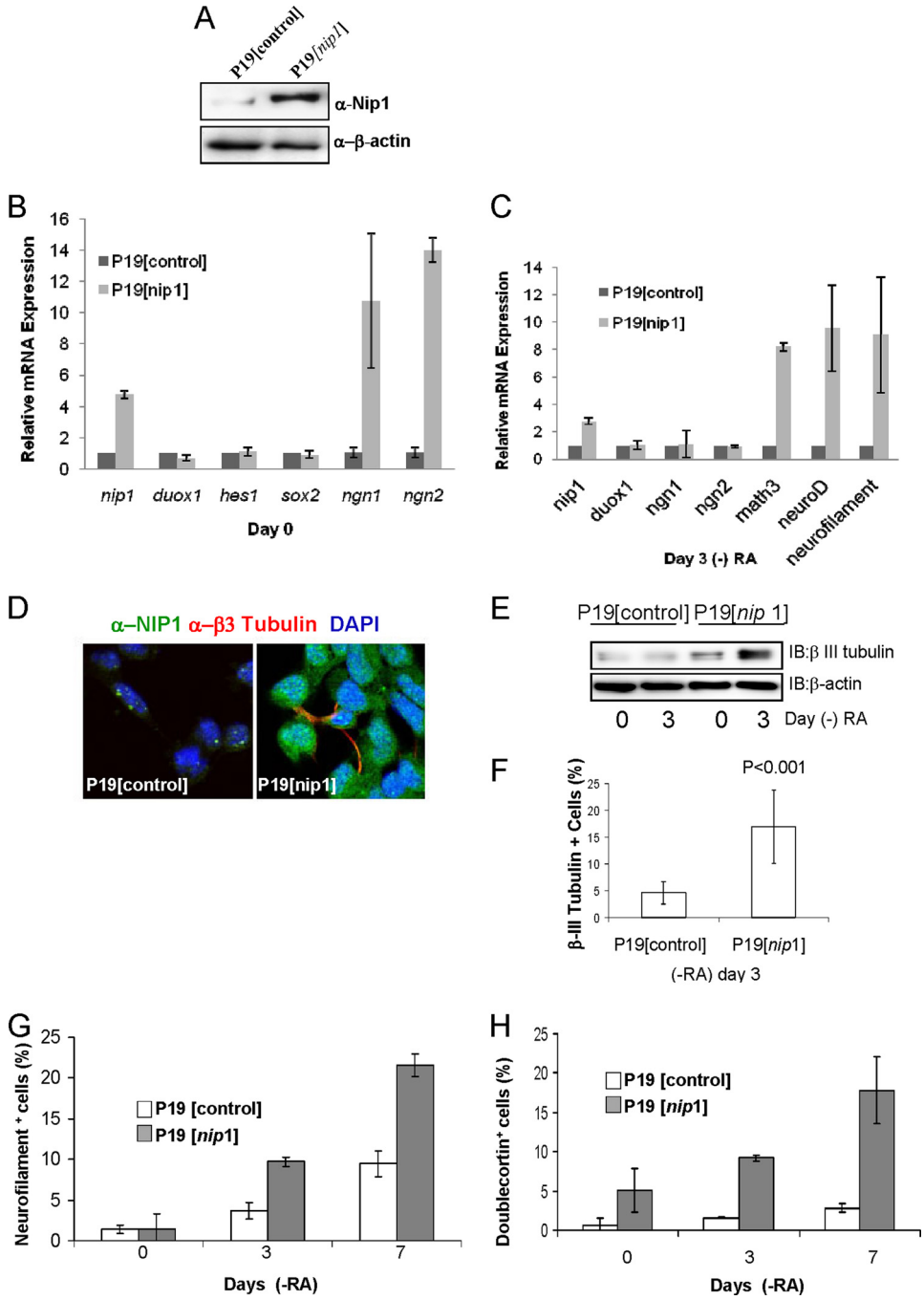

FIGURE 3. **Ectopic expression of Nip1 results in induction of neuronal differentiation in P19 cells.** *A*, shown is an anti-Nip1 Western blot showing enhanced Nip1 level in P19 cells stably transfected with a *nip1-myc* expression vector. *B*, a comparison is shown of expression levels between P19[*nip1*] clones and P19 control cells for *nip1*, *duox1*, *hes*, *sox2*, *neurogenin1*, and *neurogenin 2* before differentiation. *C*, shown is a comparison of expression levels between P19[*nip1*] clones and P19 control cells for *nip1*, *duox1*, *neurogenin1*, *neurogenin 2*, *math3*, *neuroD*, and *neurofilament* on day 3 of differentiation in the absence of RA. Graphs were based on qRT-PCR data. Expression levels were normalized to that of glyceraldehyde-3-phosphate dehydrogenase. An *error bar* represents the S.D. of two independent experiments. *D*, P19[*nip1*] transformants or P19[control] cells were aggregated without RA. Immunofluorescence images of Anti-βIII-tubulin (*red*) and anti-Nip1 (*green*) followed by 4′,6-diamidino-2-phenylindole (*DAPI*, *blue*) staining for the nucleus in P19[*control*] and P19[*nip1*] cells on day 3 of aggregation. Magnification is 6300×. *E*, an anti-βIII-tubulin Western blot (*IB*) on days 0 and 3 of aggregation is shown. *F*, quantification of cells showing positive immunostain for β-III tubulin in P19[*nip1*] transformants or P19[control] cells on day 3 of aggregation. Cells were also immunostained for neurofilament or DCX on days 0, 3, and 7. Cells were then examined by flow cytometry to evaluate the populations of cells that expressed neurofilament (*G*) or DCX (*H*); **, $p < 0.001$ *versus* P19[control]. An *error bar* represents the S.D. of three-five independent experiments.

of an inducing chemical (Fig. 2*H*). We employed qRT-PCR to assess the temporal pattern of the *nip1* transcript during RA-induced neuronal differentiation of P19 cells. Compared with undifferentiated P19 cells on day 0, RA treatment led to a transient increase in *nip1* mRNA on day 2 (Fig. 2*F*). This corresponded to the time point at which proneural genes such as *neurogenin* and *neuroD* were up-regulated (Fig. 2*I*) but preceded the up-regulation of βIII-tubulin (Fig. 2*H*). Before terminal neuronal differentiation, a sharp decline in *nip*1 expression was observed (Fig. 2*F*). In a similar manner, the *nip1* transcript was up-regulated on day 4 of embryoid body formation in ES cells and subsequently down-regulated on day 6 (Fig. 2*G*). The transient up-regulation of the *nip1* transcript during neuronal differentiation of P19 and ES cells and its relatively high level of expression in NS cells are consistent with the concept that Nip1 might be involved in regulation of neuronal differentiation of stem cells.

Overexpression of nip1 in P19 Cells Induces Neuronal Differentiation—P19 cells, which express a low basal level of *nip*1 (Fig. 2*A*) and are relatively easy to manipulate, provide a convenient system in which to explore the function of Nip1 in cell differentiation by ectopic expression. To investigate whether forced expression of Nip1 may induce neuronal differentiation in the absence of RA, we transfected P19 cells with an expression plasmid for Myc-tagged Nip1 and isolated clones stably expressing Nip1-Myc (termed P19[*nip1*] herein). P19 cells transfected with an empty vector (or P19[control]) were used as controls. A significant increase in Nip1 expression by the P19[*nip1*] stable transformants cells was verified by an anti-Myc Western blot (not shown), anti-Nip1 Western blot (Fig. 3*A*), and by qRT-PCR analysis (Fig. 3*B*). In contrast, *duox1* mRNA level was not affected by ectopic expression of Nip1 (Fig. 3*B*). The level of expression of Numb tran-

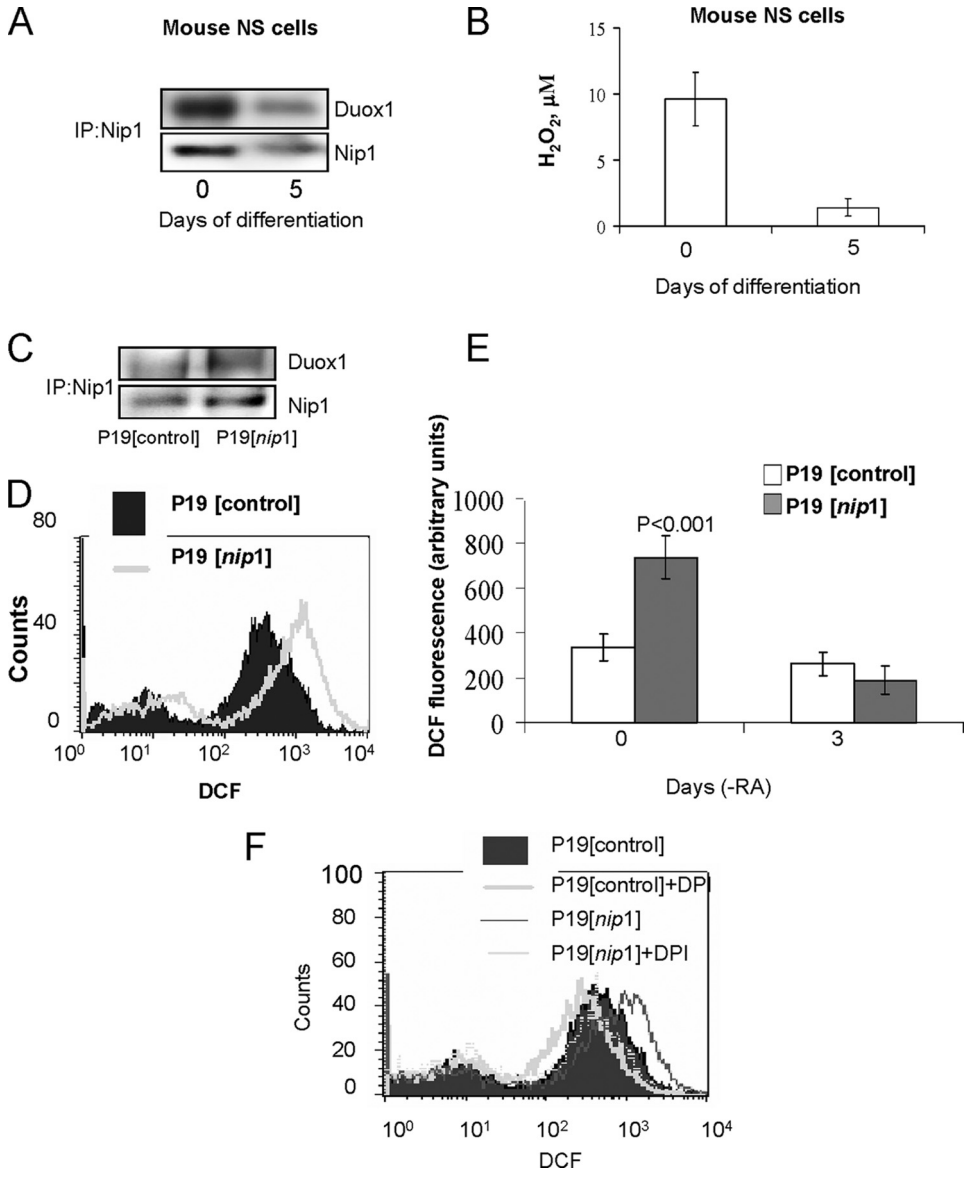

FIGURE 4. **Undifferentiated NS cells and P19[nip1] stable transformants display enhanced levels of intracellular ROS.** *A*, a Western blot shows coimmunoprecipitation (*IP*) of Nip1 and Duox1 on day 0 and day 5 of NS cell differentiation. *B*, shown is quantification of ROS production in neuronal stem cells undergoing differentiation. Release of hydrogen peroxide was detected using Amplex Red; **, $p < 0.001$ *versus* day 0. Statistics were Student's *t* test. *C*, a Western blot shows co-immunoprecipitation of Nip1 and Duox1 in P19[nip1] transformants and P19[control] cells on day 0. *D*, representative flow cytometry histogram shows the distribution of DCF fluorescence in clonal population of P19[*nip1*] transformants and P19[control] cells on day 0. *E*, the H_2O_2 concentration was measured by incubating cells with 2′,7′-dichlorodihydrofluorescein diacetate followed by flow cytometry gated on DCF fluorescence. An *error bar* represents the S.D. of 3–5 independent experiments; **$p < 0.001$ compared with P19[control]. Statistics were Student's *t* tests. *F*, a representative flow cytometric histogram shows ROS levels assessed by DCF staining in P19[*nip1*] and P19 [control] clones treated or not with diphenyleneiodonium chloride (*DPI*) for 30 min. The histogram is representative of three independent analyses.

scripts was also not affected by up-regulation of Nip1 in P19 cells, and the protein distribution patterns varied from each other (supplemental Fig. S1, *B* and *C*). Increased Nip1 expression in P19[*nip1*] cells corresponded to elevated levels of *neurogenin1* and *neurogenin2* transcripts on day 0. No differences were observed for the *hes1* and *sox2* transcripts between the P19[*nip1*] and control cells (Fig. 3*B*). On day 3 of aggregation, the P19[*nip1*] clones exhibited elevated expression of *math3* (8 ± 0.2-fold), *neuroD* (10 ± 3-fold), and *neurofilament* (9 ± 4-fold) in comparison to the P19[control] cells (Fig. 3*C*). A decrease in *neurogenin1* and *neurogenin2* mRNA was noted in the P19[*nip1*] clones on day 3, as compared with day 0. Sustained levels of *nip1* mRNA on days 0 and 9 in P19[nip1] clones was verified by Northern blot analysis (supplemental Fig. S1*C*). In contrast, no change was observed for *Duox1* mRNA in the P19[*nip1*] compared with control clones between day 0 and day 3 of aggregation. These data indicate that the neurogenic program had been initiated by ectopic expression of Nip1 on day 0, independently of RA.

Next we immunostained cells on day 0 and post-aggregation days 3 and 7, aggregated in the absence of RA for the neuronal-specific structural proteins βIII-tubulin, Neurofilament, and Doublecortin (DCX). Cells were examined for βIII-tubulin by immunofluorescence (Fig. 3*D*), Western blot (Fig. 3*E*), and flow cytometry (Fig. 3*F*) to monitor neuronal differentiation after aggregation. Overexpression of Nip1 in P19[*nip1*] cells significantly increased the expression of βIII-tubulin (Fig. 3*F*). Flow cytometry showed that 17 ± 6.8% of P19[*nip1*] clones exhibited immunoreactivity to anti-βIII-tubulin compared with 4.7 ± 2% for the P19[control] cells (Fig. 4*E*). The P19[*nip1*] cells showed a 25% increase in immunostaining for neurofilament relative to controls (9 ± 1.6%) as measured by flow cytometry (Fig. 3*G*). Analysis of DCX by flow cytometry demonstrated that by day 7 of post-aggregation, ~3% of P19[control] cells stained positive for doublecortin. In contrast, 9.2 ± 1.6% of P19[*nip1*] transformants were DCX-positive on day 3 of aggregation, and this number approached 20% (18 ± 2.8) by day 7 (Fig. 4*F*). The increases in the expression of neuronal structural proteins are consistent with qRT-PCR results (Fig. 3*B*). Together these data suggest that ectopic Nip1 expression leads to the acquisition of precocious neuronal fate in P19 cells in the absence of RA with or without aggregation and promotes neural differentiation upon aggregation.

Nip1-mediated Neuronal Differentiation Is Associated with Duox-mediated ROS Generation—To elucidate the mechanism of Nip1-induced neuronal differentiation, we examined Duox

expression in primary NS cells. Co-expression of Doux1 and Nip1/Douxa1 in cells was shown to be critical for generation of ROS (17). In agreement with the literature (17, 36), we show that Nip1 and Duox1 formed a complex in mouse NS cells (Fig. 4*A*). Interestingly, both the protein level and interaction of the two proteins decreased upon differentiation, coinciding with marked reduction in the intracellular concentration of hydrogen peroxide, which decreased to ⅕ that of the basal level by day 5 of differentiation (Figs. 4, *A* and *B*). These data suggest that dual oxidase maturation is tightly regulated during NS cell differentiation and that ROS may play a role in initiating neuronal differentiation.

To confirm the above finding, we measured ROS generation in the P19[*nip1*] clones that were shown to differentiate into neurons in an autonomous fashion (Fig. 3). We verified that Duox1 was localized to the plasma membrane along with Nip1 (supplemental Fig. S1*B*) and that a protein complex containing Nip1 and DUOX1 existed in P19[nip1] cells (Fig. 4*C*). To validate the presence of functional Duox1, we measured the intracellular ROS levels in P19[*nip1*] and P19[control] cells. We found that undifferentiated P19[*nip1*] clones consistently produced significantly higher levels of ROS than the P19[control] cells (Fig. 4, *D* and *E*). To obtain further evidence that the elevated ROS production observed in the P19[*nip1*] cells was mediated by the Nip1-Doux1 pathway, we treated the P19[*nip1*] cells with diphenyleneiodonium chloride, a broad NADPH oxidase inhibitor (37). Diphenyleneiodonium chloride treatment of the P19[*nip1*] cells brought the intracellular ROS to a level slightly below that observed in the untreated P19[control] cells (Fig. 4*F*). Although Duox1 and Duox2 function as efficient H_2O_2 generators on the cell surface, they may also produce superoxide like other members of the NADPH oxidase family (12, 14, 36, 38). We, therefore, evaluated the intracellular superoxide levels for the different P19 clones before or 3 days after aggregation in the absence of RA using hydroethidine as a probe. The P19[*nip1*] clones showed an increase in intracellular superoxide formation relative to the control (Fig. 5*A*). However, the superoxide production was reduced on day 3 of differentiation relative to day 0. We treated the P19[*nip1*] or control cells with the catalytic antioxidant manganese(III) *meso*-tetrakis(4-benzoic acid) porphyrin (MnTBAP) to attenuate the effect of superoxide (39) and aggregated the cells in the absence of RA to examine its effect on neuronal differentiation using neurofilament as a marker. As shown in Fig. 5*B* by qRT-PCR analysis, whereas MnTBAP had little effect on the P19[control] cells, it led to a decrease in neurofilament expression in P19[*nip1*] cells. Quantification of neurofilament-positive cells confirmed that neuronal differentiation was significantly reduced (28 ± 2%, $p < 0.05$) in MnTBAP-treated cells, suggesting that superoxide was only partially involved in regulation of Nip1-induced neuronal differentiation (Fig. 5, *B* and *C*). Together these data suggest that Nip1 may at least in part control the progress of neuronal differentiation in stem cells through Nip1-Duox1-mediated ROS production.

Depletion of Nip1 Expression in P19 Cells Leads to Impaired Neuronal Differentiation—The function of endogenous Nip1 in P19 cells was examined using a Nip1-specific shRNA. P19 cells were transiently transfected with plasmids expressing

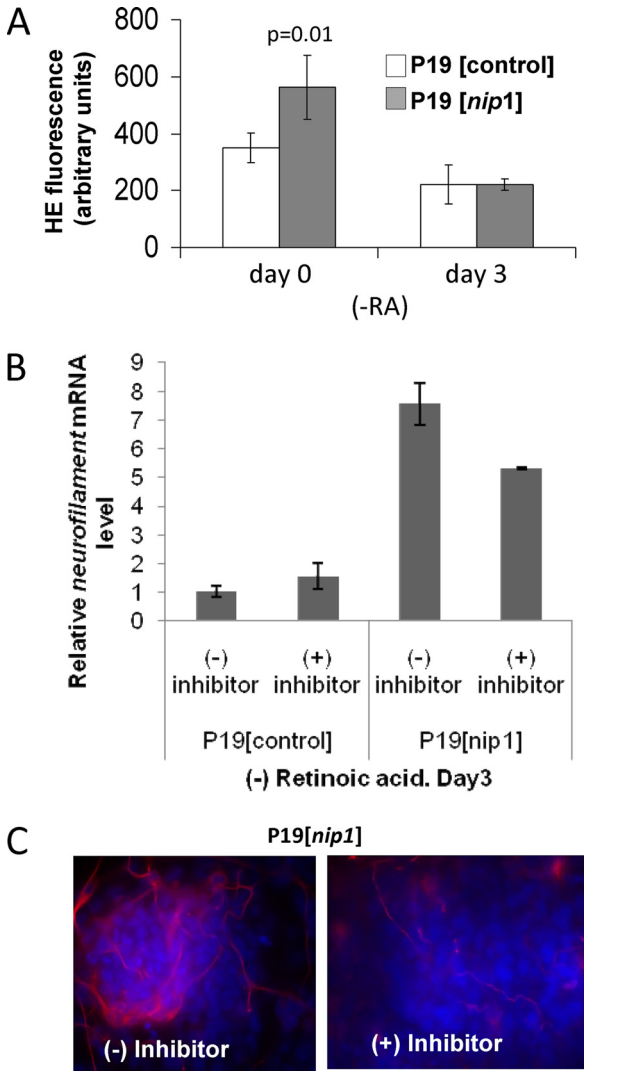

FIGURE 5. **Enhanced superoxide levels contribute to neuronal differentiation of P19[nip1] stable transformants.** *A*, shown is quantification of hydroethidine (*HE*) fluorescence in P19[*nip1*] transformants *versus* control cells at days 0 and 3 of aggregation. An *error bar* represents the S.D. of data obtained from three P19[*nip1*] clonal populations; *, $p < 0.01$ *versus* P19[control]. *B*, a qRT-PCR analysis shows the effect of MnTBAP on the neurofilament mRNA transcript level in P19[*nip1*] and P19[control] cells on day 3 of aggregation without RA. *C*, a representative neurofilament immunofluorescence image shows the inhibitory effect of MnTBAP on neurogenesis by P19[*nip*1] cells. Images were obtained from cells on day 7 of aggregation. Magnification is 400×.

a *nip1*-specific shRNA or a scrambled shRNA (scrRNA) (supplemental Fig. S4, *C* and *D*). These cells were co-transfected with a green fluorescent protein-expressing vector to monitor transfection efficiency (supplemental Fig. S4, *A* and *B*). At 24 h post-transfection, the shRNA-*nip1* cells displayed a reduction in anti-Nip1 immunostaining as compared with the scrambled controls. A 60–80% suppression of Nip1 expression was demonstrated in the Nip1 knockdown cells at 24–72 h based on quantitative PCR analysis (Fig. 6*A*). We further verified the suppression of Nip1 protein in *nip1*-specific shRNA P19 cells by flow cytometry (Fig. 6*B*) and Western blot analysis (Fig. 6*C*). These cells were aggregated in the presence of RA, and their neuronal differentiation profile was compared with that of the scrRNA cells. As shown in Fig. 6*A*, although RA was capable of

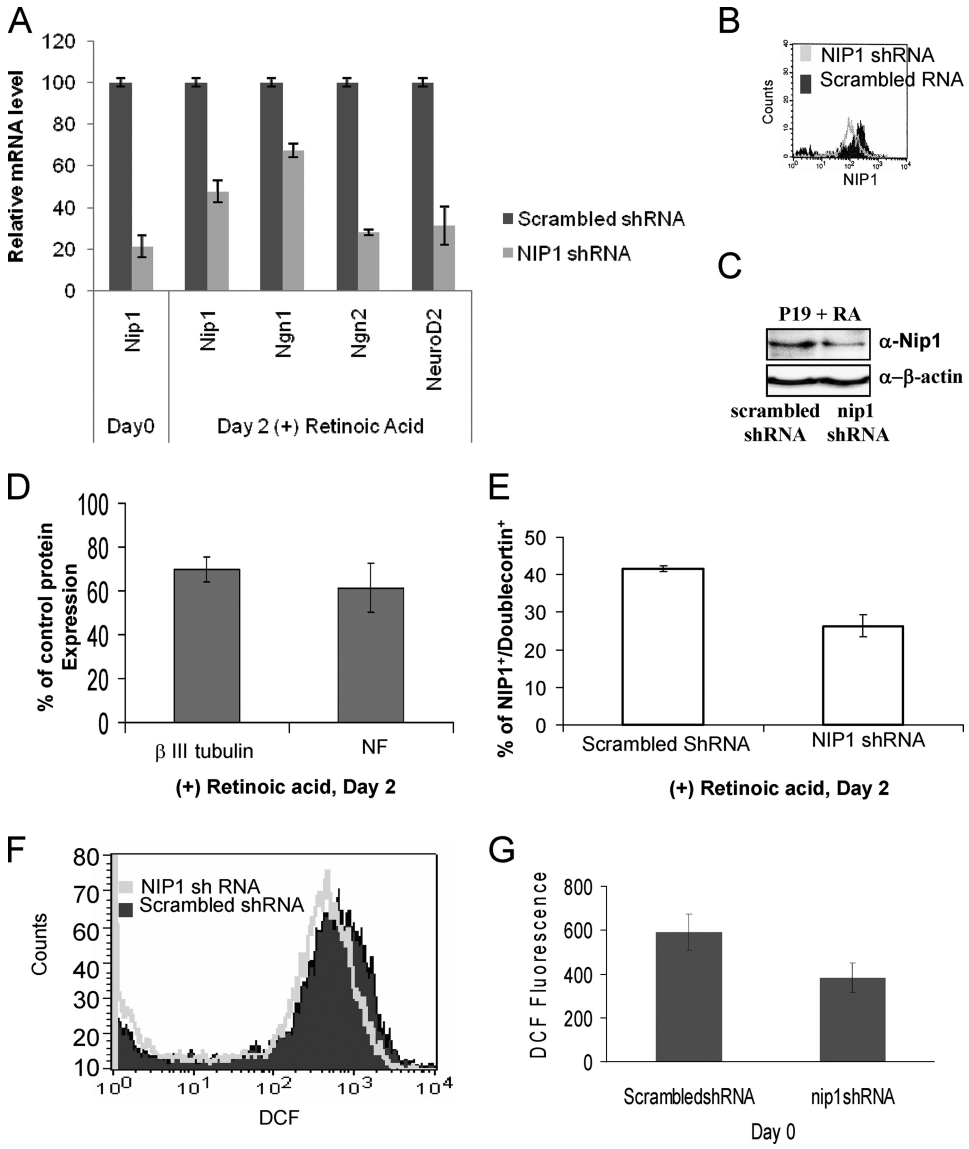

FIGURE 6. **Depletion of Nip1 leads to impairment of neuronal differentiation in P19 cells.** *A*, P19[*nip1*-shRNA] or P19[scrRNA] transfectants were aggregated with RA, and the mRNA levels of *nip1*, *neurogenin1*, *neurogenin2*, and *neuroD* were quantified by qRT-PCR on day 2. *B*, a representative flow cytometric histogram shows changes in Nip1 expression in P19 cells transiently transfected with *nip1*-specific shRNA or scrRNA. This histogram is representative of three independent analysis. *C*, shown is a Western blot analysis of Nip1 in P19[*nip*1-shRNA] or P19[scrRNA] cells. *D*, P19[*nip*1-shRNA] or P19[scrRNA] cells were aggregated in the presence of RA and assessed for neurogenesis on day 2 by immunofluorescence against βIII-tubulin or neurofilament (*NF*). Shown on the graph are the immunofluorescence in P19[*nip*1-shRNA] cells relative to the corresponding immunofluorescence signals in the P19[scrRNA] control cells; *, $p < 0.01$ *versus* P19[scrRNA]. Statistics were from Student's *t* test. *E*, shown is analysis of doublecortin expression in P19[nip1-shRNA] or P19[scrRNA] cells on day 2 of aggregation in the presence of RA. *F*, DCF fluorescence flow cytometry signals (measure of ROS) in P19[*nip*1-shRNA and P19[scrRNA] cells are shown. *G*, shown is a graphical representation of reduced ROS production in Nip1-knockdown cells. *, $p < 0.01$ *versus* P19[scrRNA]. An *error bar* represents the S.D. of three-four independent experiments.

initiating neuronal differentiation in both the P19[*nip1*-shRNA] and the P19[scrRNA] cells, marked reductions in *neurogenin1*, *neurogenin2*, and *neuroD* expression on day 2 of aggregation were observed in the former cells in comparison to the latter. Similarly, flow cytometric analysis indicated a 30–40% decrease in the number of cells that were stained positive for βIII-tubulin, neurofilament, and doublecortin on day 2 (Fig. 6, *D* and *E*, and supplemental Fig. S4*G*). The intracellular ROS production in the P19[*nip1*-shRNA] cells was decreased 30–50% compared with the P19[scrRNA] cells (Fig. 6, *F* and *G*), suggesting once again that ROS may in part be linked to the role of Nip1 in neurogenesis. The weak suppression of RA-induced neurogenesis in P19[*nip1*-shRNA] cells and the incomplete suppression of neurogenesis in P19[*nip1*] by MnTBAP suggest that RA may be able to eventually overcome the effect caused by a deficiency in Nip1 expression and function and that there are other factors involved in the neurogenic phenotype of these cells.

Overexpression of Nip1 Causes Cytoskeleton Reorganization—To gain further molecular insight into the neuronal differentiation induced by Nip1 in P19 cells, we combined transcriptomic and proteomic techniques to identify targets with differential expression between P19[*nip1*] and P19[control] cells aggregated for 3 days in the absence of RA. Using cDNA microarray analysis (see supplemental Table 2), numerous changes in the expression of cell cycle-related genes, development and transcription genes, and cytoskeleton genes were reproducibly detected. There was up-regulation of transcripts of class II intermediate filament proteins, periferin and vimentin, and actin-binding proteins involved in the anchoring of actin, dynamic turnover, and restructuring of the actin cytoskeleton such as profilin 1 dystonin and oligophrenin 1 (Fig. 7*A*). Interestingly, dystonin is essential for maintaining neuronal cytoskeleton organization and, along with peripherin and oligophrenin, is also involved in anchoring neural intermediate filaments to the actin cytoskeleton in axonal growth cones (40–42). Furthermore, in agreement with our data and the data of others showing a pivotal role for the Nip proteins in the generation of ROS, among the differentially expressed genes in Nip1-overexpressing cells, a significant increase was detected for several regulators of the cellular redox state such as selenoprotein and metallothionein 1 (supplemental Table 2).

The mass spectrometry (MS) analysis of P19[*nip1*] cells revealed that Nip1 may form complexes with proteins related to cytoskeleton organization, such as actin, vimentin, tropomyosin, and lamins A/C, and proteins involved in chromatin organization, such as histones H4 and 2A (Fig. 7*B*). The expression of lamin A/C was analyzed in more detail, as lamin proteins are among major structural nuclear proteins that affect nuclear

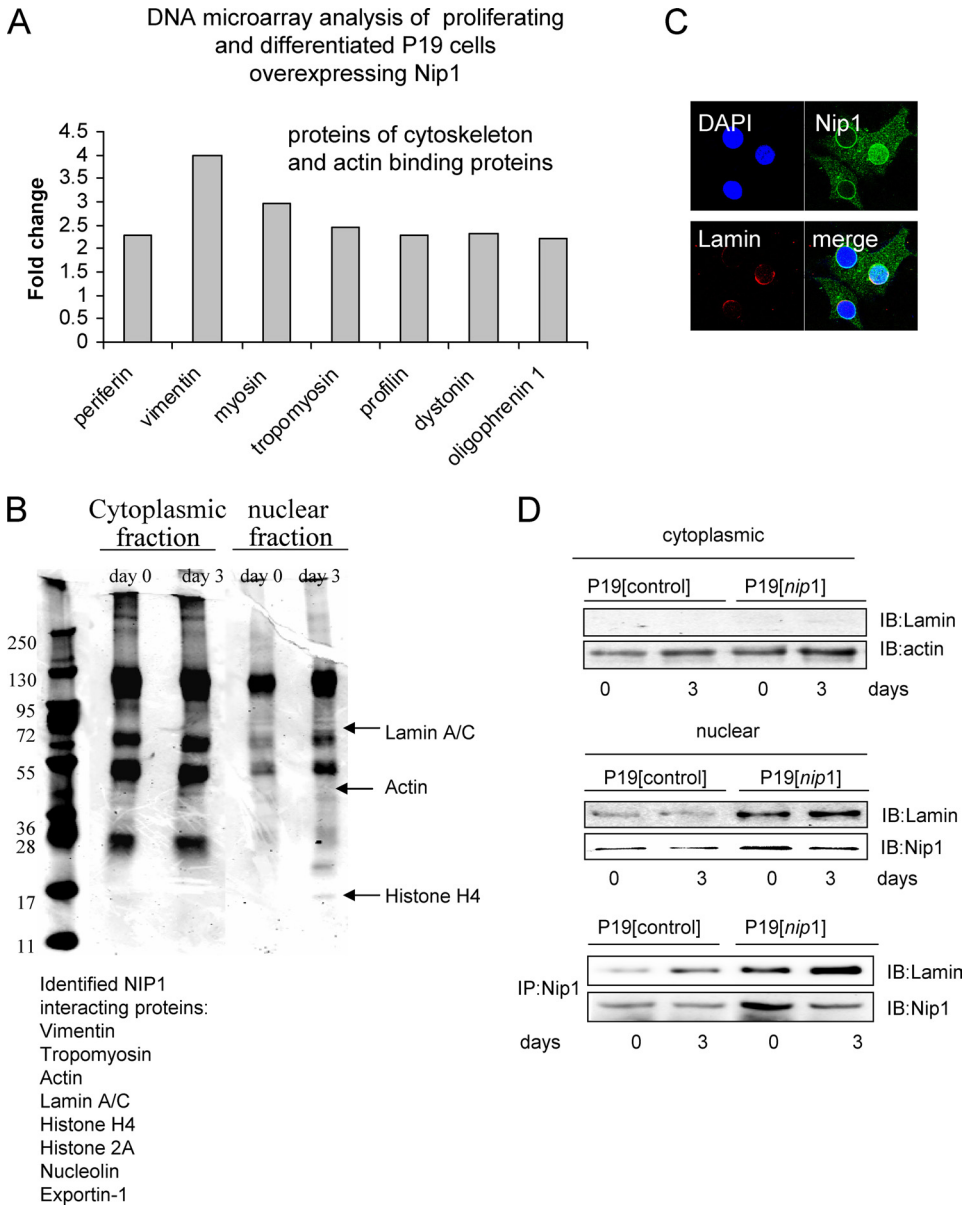

FIGURE 7. **Identification of transcriptional targets and interaction partners of Nip1 in P19 cells.** *A*, shown is an increase in expression of transcripts associated with cytoskeleton in differentiating P19[*nip1*] and P19[control] cells as measured by DNA microarray analysis. Genes that were 2-fold or more up-regulated and had a p value <0.05 by t test were identified as significantly changed. *B*, Nip-1 immunoprecipitates were resolved by one-dimensional electrophoresis and stained with Coomassie Brilliant Blue. Bands were cut out and subjected to in-gel trypsin digestion before mass spectrometric analysis. *C*, Nip1 and lamin A/C were co-expressed and co-localized in P19 cells overexpression Nip1. Cells were immunostained with anti-Nip-1 (*green*) and anti-lamin A/C (*red*) followed by 4′,6-diamidino-2-phenylindole (DAPI, *blue*) staining for nuclear. *D*, Western blot analysis (*IB*) is shown of lamin A/C in nuclear extracts of undifferentiated and differentiated P19[nip1] and P19[control] cells. Magnification is 6300×. Coimmunoprecipitation of lamin A/C and Nip1 was examined in vector control and Nip1-overexpressing P19 cells at day 0 and day 3 of differentiation in the absence of RA. The cell extracts were immunoprecipitated (*IP*) with anti-Nip1 antibody and probed with antibodies to lamin A/C.

integrity and function. Lamin A/C immunofluorescence was seen to overlap with that of Nip1, indicating that these two proteins co-localized in P19[*nip1*] cells (Fig. 7*C*). Increased expression of Nip-1 in both non-differentiated and differentiated P19 cells stably expressing Nip1 was associated with an increase in lamin A/C expression and the formation of complexes between Lamin A/C and Nip1(Fig. 7*D*). To further verify that the reorganization of lamin A/C is important for Nip1-mediated differentiation, we examined P19 cells transiently transfected with plasmids expressing a lamin A/C-specific shRNA. Suppression of lamin A/C was verified by Western blot analysis (Fig. 8*C*). It was shown earlier that suppression of Nip decreased the number of cells that were stained positive for doublecortin (Fig. 6*E*). We show further that suppression of Nip1 diminished the number of cells stained positive for both lamin and doublecortin. However, suppression of both Nip1 and lamin A/C did not further decrease the expression of doublecortin (Fig. 8*A*). Therefore, doublecortin acts upstream of Nip1 but not lamin A/C in the acquisition of neuronal fate. Suppression of lamin A/C diminished βIII-tubulin staining by 40% in P19[*nip*1] cells, whereas it did not affected differentiation of P19[control] cells (Fig. 8, *B* and *C*). These results indicate that lamin A/C is regulated by Nip1 and is involved in Nip1-mediated neuronal differentiation. Taken together, our results indicate that the effect of Nip1 up-regulation on neuronal differentiation could be explained by modulation of proteins related to cytoskeleton organization, in particular components of nuclear lamina, which control the development of neuronal types. We propose a model for Nip1-induced neurogenesis in which an increase in Nip1 expression in pluripotent stem cells leads to neuronal cell fate determination (Fig. 8*D*). This is in part due to an increase in intracellular ROS production, likely through activation of Duox1. However, our data also suggest that there are other mechanisms related to nuclear lamina and cytoskeleton reorganization underlying the Nip1-induced stimulation of differentiation.

DISCUSSION

We describe here a novel function for Nip1 as an intrinsic regulator of neuronal cell fate in stem cell differentiation. The *nip1* transcripts were first detected in adult brain. During mouse brain development, the expression of Nip1 was highly evident from the early stages (E10.5) throughout differentiation. Forced expression of Nip1 in pluripotent P19 cells up-regulated expression of proneuronal factors, associated with high level of lamin A/C expression, and facilitated differentiation into neuronal cell types that exhibited higher levels of immunoreactivity for the neuronal cytoskeletal pro-

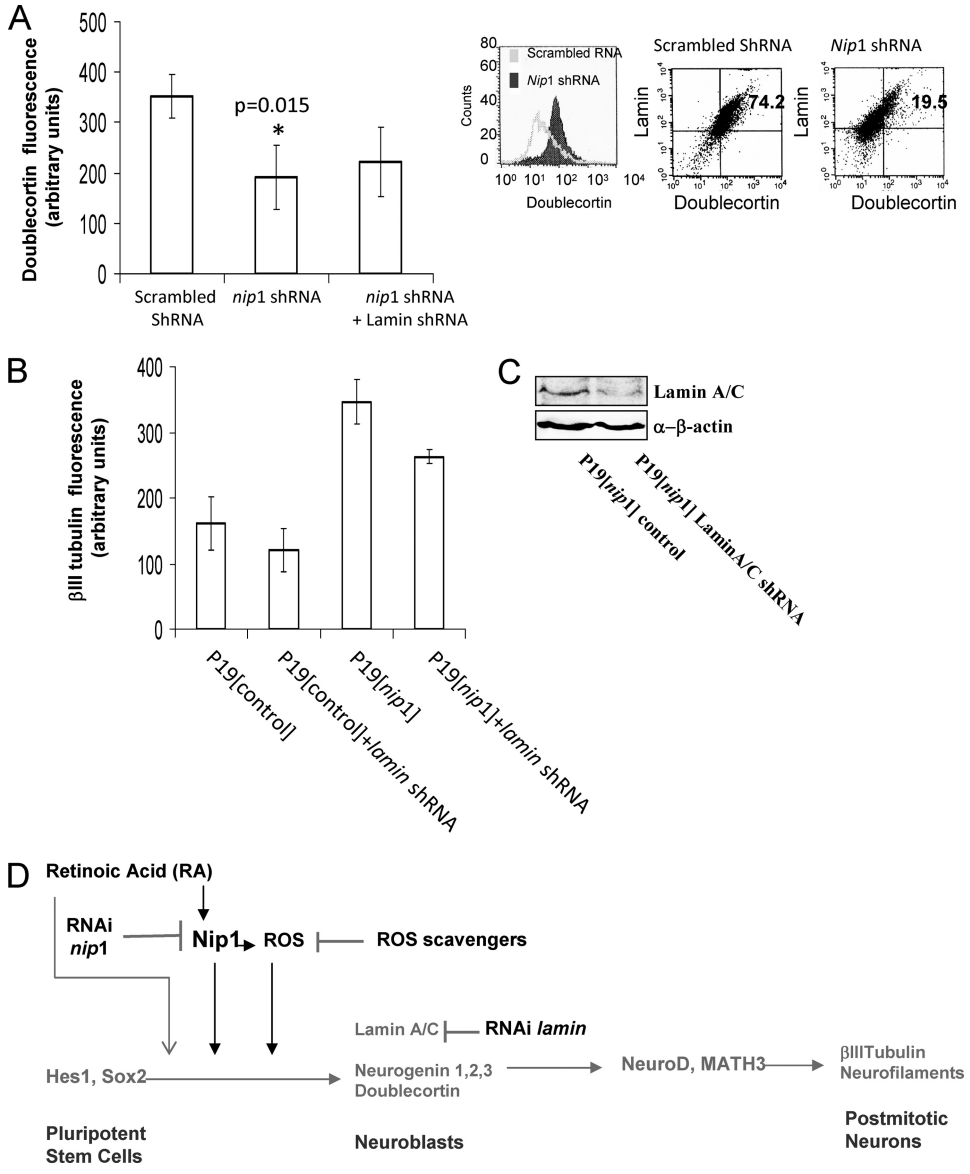

FIGURE 8. **The role of lamin A/C in Nip1 mediated neuronal differentiation.** *A*, P19 cells show a decrease in expression of doublecortin in P19 cells transfected with *nip1*-specific shRNA, lamin A/C-specific shRNA, or a scrambled shRNA. A representative flow cytometric histogram shows changes in lamin A/C and doublecortin expression in P19[*nip*1-shRNA and P19[scrRNA] cells. These histograms are representative of three independent analyses. *B*, changes in βIII tubulin expression in P19[*nip1*] and P19[control] cells transiently transfected with lamin A/C-specific shRNA or a scrambled shRNA are shown. *C*, shown is a Western blot analysis of lamin A/C. *D*, shown is a proposed model of regulation of Nip1-mediated differentiation.

teins doublecortin, βIII-tubulin, and neurofilament when aggregated in the absence of retinoic acid. Our data show that DuoxA1 expression in stem cells is not restricted to cytoplasmic compartments, in contrast to reports for epithelial HeLa cells (17). We showed that Nip1 was required for proper expression of proneuronal genes as depletion of endogenous Nip1 expression caused decreases in the *neurogenin1*, *neurogenin2*, and *neuroD* transcripts in P19 cells treated with RA to induce neuronal differentiation.

Nip1 (Duoxa1) was linked to regulation of Duox1 and, thereby, ROS production in cells (17). Duox was originally described to regulate iodide oxidation during the biosynthesis of thyroid hormones (13–15). However, Duox enzymes and their maturation factors are not restricted to the thyroid tissue. Interestingly, although basal Nip1 levels in P19 EC cells is magnitudes lower than that reported in the thyroid, its expression was elevated when cells were aggregated with RA (17, 43).

ROS including superoxide ($O_2^{\cdot-}$) and hydroxyl ($^{\cdot}OH$) radicals and hydrogen peroxide (H_2O_2) have been shown to regulate a number of cellular processes such as growth, differentiation, and neurotransmission. Although elevated ROS production has been associated with neuronal cell death, recent studies suggest that ROS may play a role in neuronal differentiation (44). Nerve growth factor-induced neuronal differentiation of PC12 cells has been shown to be mediated by an increase in H_2O_2 (45–47). Treatment of PC12 cells with either nicotinamide adenine dinucleotide phosphate (NADPH) oxidase inhibitor, diphenylene iodonium, catalase, or *N*-acetylcysteine negated the nerve growth factor response and blocked neuronal differentiation (45, 48). Furthermore, NADPH oxidase has been implicated in hippocampal long term potentiation, neuronal growth cone formation, and neurite outgrowth (49, 50). However, Tsatmali *et al.* (51) showed that ROS production does not influence the probability of a cell becoming a neuron during development. These apparent contradictions suggest that there could be factors other than NADPH oxidase 1 that control the cellular level of ROS during neuronal differentiation and development. In accordance with a role for Nip1 in ROS generation, we found that ROS were elevated in P19[*nip1*] cells and diminished in Nip1-knocked-down cells. The increase in ROS generation was comparable with the level of endogenous ROS elevation associated with embryonic stem cell differentiation (52).

Tissue-restricted NS cells also expressed a high level of Nip1. The observed reduction in ROS production in differentiated NS cells is consistent with previous observations showing an increase in ROS generation in E15 and E17 mouse cortex followed by a strong decline in ROS concentration from E21 through P12 (53). Thus, although ROS are required for early steps of neuronal differentiation, mature neurons are particularly susceptible to ROS-induced cell damage, necessitating low levels of ROS in these cells (54). Consistent with changes in ROS generation, significant dynamic alterations occur during

neuronal development in enzymatic systems involved in protection against oxidative stress. Thus, catalase activity increases in developing neurons and decreases upon neuronal maturation to reduce exposure of post-mitotic neurons to ROS.

The Nip1 protein was originally identified based on its ability to bind Numb. Numb has been shown to play a pivotal role in neurogenesis in both *Drosophila* and mouse (55–58). However, our findings showed that distribution of Numb differed from that of Nip1 in developing brain and P19 cells overexpressing Nip1 and Numb. Furthermore, up-regulation of Nip1 did not affect the regulation of Numb in P19 cells. Overexpression of Numb in P19 cells promotes neuronal differentiation but only in the presence of RA (55). Because forced expression of Nip1 in P19 cells induced neuronal differentiation in the absence of RA, it is evident that Nip1 and Numb play distinct roles in neurogenesis. This is supported by the fact that the expression of Numb remained essentially unchanged during RA-induced neuronal differentiation of P19 cells (supplemental Fig. S3*B*), whereas the *nip1* transcript underwent a 5-fold change from day 1 to day 2 of aggregation (Fig. 2*E*).

Cytoskeletal re-arrangements elaborated during development have a major impact on function of neuronal cells (59, 60). Our microarray data showed that during differentiation, Nip1 overexpression stimulated induction of genes encoding neuronal intermediate filament proteins and actin-binding proteins that are expressed in the developing mammalian nervous system proteins. For example, profilin and dystonin identified as actin-binding proteins were linked to neuronal differentiation and synaptic plasticity (61). Vimentin is expressed by neuronal precursors, and its expression declines in the immature neurons (62), whereas peripherin is the major neuronal intermediate filament that is most abundant in the peripheral nerve system (63). Mass spectrometry analysis of Nip1 immunoprecipitates identified new potential Nip1 partners, among them lamin A/C. Lamin A/C is not observed in undifferentiated or proliferative cells, but its expression is activated in neuronal lineages and cardiomyocytes differentiated from human embryonic stem cells and in all mature and nearly mature neurons (22, 25, 64, 65). Previously, it has been shown that undifferentiated P19 pluripotent mouse embryonal carcinoma cells contain low steady-state levels of lamins A/C RNAs that begin to increase 48 h after treatment with retinoic acid (23, 66). These earlier reports nicely complement our observation that lamin-A/C is expressed in Nip1-expressing P19 cells showing accelerated differentiation into neuronal lineage even in the absence of retinoic acid. The importance of lamins is defined by their ability to provide connection to other proteins involved in maintenance of nuclear structure and proteins that are involved in DNA replication and transcription (21, 67). The complex formation between lamin A/C and Nip1 may have a unique regulatory function in acquiring a specific stage during differentiation. Our findings suggest that changes in lamin A/C expression is part of the overall changes after up-regulation of Nip1 during neuronal differentiation, and these changes could constitute an important regulator of cell fate determination.

In summary, Nip1 expression in pluripotent stem cells leads to neuronal cell fate determination. This is in part due to an increase in intracellular ROS production (Fig. 5, *A*), likely through activation of Duox1 (Fig. 5*C*), and modulation of cytoskeleton organization, in particular nuclear A-types lamins (Fig. 7, *A–D*). Poor efficiency of ROS inhibitors in Nip1-induced neuronal differentiation indicates that the primary role of Nip1 in stem cell differentiation might be in its ability to modulate cytoskeleton organization or via other yet unknown mechanisms underlying the stimulation of differentiation observed. Our findings on the role of Nip1 in neurogenesis and neuronal differentiation are summarized in the model depicted in Fig. 8*D*. Future studies aimed at achieving controlled neuronal differentiation by altering Nip1 expression in embryonic or induced stem cells may provide insights into the understanding, diagnosis, and treatment of neurodevelopment disorders and neurodegenerative diseases.

Acknowledgments—We thank Dr. Josee Savage for providing the scrambled shRNA plasmid and for helpful discussions. We thank Paula P. Pittock, University of Western Ontario Biological Mass Spectrometry Laboratory, for running the mass spectrometry samples. We thank Linda Jackson-Boeters, University of Western Ontario Department of Pathology, for help with the immunohistochemistry. We are grateful to Dr. Q. Feng for providing access to facilities for carrying out quantitative PCR analysis.

REFERENCES

1. Johnson, J. E., Birren, S. J., and Anderson, D. J. (1990) *Nature* **346,** 858–861
2. Guillemot, F., Lo, L. C., Johnson, J. E., Auerbach, A., Anderson, D. J., and Joyner, A. L. (1993) *Cell* **75,** 463–476
3. Akazawa, C., Ishibashi, M., Shimizu, C., Nakanishi, S., and Kageyama, R. (1995) *J. Biol. Chem.* **270,** 8730–8738
4. Ma, Q., Kintner, C., and Anderson, D. J. (1996) *Cell* **87,** 43–52
5. Sommer, L., Ma, Q., and Anderson, D. J. (1996) *Mol. Cell. Neurosci.* **8,** 221–241
6. Kageyama, R., Ohtsuka, T., Hatakeyama, J., and Ohsawa, R. (2005) *Exp. Cell Res.* **306,** 343–348
7. Lazarides, E. (1980) *Nature* **283,** 249–256
8. Moody, S. A., Quigg, M. S., and Frankfurter, A. (1989) *J. Comp. Neurol.* **279,** 567–580
9. Francis, F., Koulakoff, A., Boucher, D., Chafey, P., Schaar, B., Vinet, M. C., Friocourt, G., McDonnell, N., Reiner, O., Kahn, A., McConnell, S. K., Berwald-Netter, Y., Denoulet, P., and Chelly, J. (1999) *Neuron* **23,** 247–256
10. Carlén, M., Cassidy, R. M., Brismar, H., Smith, G. A., Enquist, L. W., and Frisén, J. (2002) *Curr. Biol.* **12,** 606–608
11. Staines, W. A., Morassutti, D. J., Reuhl, K. R., Ally, A. I., and McBurney, M. W. (1994) *Neuroscience* **58,** 735–751
12. Geiszt, M., Witta, J., Baffi, J., Lekstrom, K., and Leto, T. L. (2003) *FASEB J.* **17,** 1502–1504
13. Dupuy, C., Ohayon, R., Valent, A., Noël-Hudson, M. S., Dème, D., and Virion, A. (1999) *J. Biol. Chem.* **274,** 37265–37269
14. De Deken, X., Wang, D., Dumont, J. E., and Miot, F. (2002) *Exp. Cell Res.* **273,** 187–196
15. Corvilain, B., van Sande, J., Laurent, E., and Dumont, J. E. (1991) *Endocrinology* **128,** 779–785
16. Qin, H., Percival-Smith, A., Li, C., Jia, C. Y., Gloor, G., and Li, S. S. (2004) *J. Biol. Chem.* **279,** 11304–11312
17. Grasberger, H., and Refetoff, S. (2006) *J. Biol. Chem.* **281,** 18269–18272
18. Nixon, R. A., and Shea, T. B. (1992) *Cell Motil. Cytoskeleton* **22,** 81–91
19. Vlcek, S., and Foisner, R. (2007) *Curr. Opin. Cell Biol.* **19,** 298–304
20. Hutchison, C. J., and Worman, H. J. (2004) *Nat. Cell Biol.* **6,** 1062–1067
21. Spann, T. P., Goldman, A. E., Wang, C., Huang, S., and Goldman, R. D. (2002) *J. Cell Biol.* **156,** 603–608

22. Constantinescu, D., Gray, H. L., Sammak, P. J., Schatten, G. P., and Csoka, A. B. (2006) *Stem Cells* **24,** 177–185
23. Lanoix, J., Skup, D., Collard, J. F., and Raymond, Y. (1992) *Biochem. Biophys. Res. Commun.* **189,** 1639–1644
24. Lebel, S., Lampron, C., Royal, A., and Raymond, Y. (1987) *J. Cell Biol.* **105,** 1099–1104
25. Röber, R. A., Weber, K., and Osborn, M. (1989) *Development* **105,** 365–378
26. Takamori, Y., Tamura, Y., Kataoka, Y., Cui, Y., Seo, S., Kanazawa, T., Kurokawa, K., and Yamada, H. (2007) *Eur. J. Neurosci.* **25,** 1653–1662
27. Skerjanc, I. S., Petropoulos, H., Ridgeway, A. G., and Wilton, S. (1998) *J. Biol. Chem.* **273,** 34904–34910
28. Yu, Y. T., Breitbart, R. E., Smoot, L. B., Lee, Y., Mahdavi, V., and Nadal-Ginard, B. (1992) *Genes Dev.* **6,** 1783–1798
29. Savage, J., Conley, A. J., Blais, A., and Skerjanc, I. S. (2009) *Stem Cells* **27,** 1231–1243
30. Rudnicki, M. A., and McBurney, M. W. (1987) in *Teratocarcinomas and Embryonic Stem Cells; A Practical Approach* (Robertson, E. J., ed) pp. 19–49, IRL Press at Oxford University Press, Oxford
31. Kennedy, K. A., Porter, T., Mehta, V., Ryan, S. D., Price, F., Peshdary, V., Karamboulas, C., Savage, J., Drysdale, T. A., Li, S. C., Bennett, S. A., and Skerjanc, I. S. (2009) *BMC Biol.* **7,** 67
32. Rietze, R. L., and Reynolds, B. A. (2006) *Methods Enzymol.* **419,** 3–23
33. Caviness, V. S., Jr., Takahashi, T., and Nowakowski, R. S. (1995) *Trends Neurosci.* **18,** 379–383
34. Ishibashi, M., Moriyoshi, K., Sasai, Y., Shiota, K., Nakanishi, S., and Kageyama, R. (1994) *EMBO J.* **13,** 1799–1805
35. Beddington, R. S., Rashbass, P., and Wilson, V. (1992) *Dev. Suppl.* 157–165
36. Morand, S., Ueyama, T., Tsujibe, S., Saito, N., Korzeniowska, A., and Leto, T. L. (2009) *FASEB J.* **23,** 1205–1218
37. Hancock, J. T., and Jones, O. T. (1987) *Biochem. J.* **242,** 103–107
38. Ameziane-El-Hassani, R., Morand, S., Boucher, J. L., Frapart, Y. M., Apostolou, D., Agnandji, D., Gnidehou, S., Ohayon, R., Noël-Hudson, M. S., Francon, J., Lalaoui, K., Virion, A., and Dupuy, C. (2005) *J. Biol. Chem.* **280,** 30046–30054
39. Laurent, A., Nicco, C., Chéreau, C., Goulvestre, C., Alexandre, J., Alves, A., Lévy, E., Goldwasser, F., Panis, Y., Soubrane, O., Weill, B., and Batteux, F. (2005) *Cancer Res.* **65,** 948–956
40. Faussone-Pellegrini, M. S., Matini, P., and DeFelici, M. (1999) *Anat. Embryol.* **199,** 459–469
41. Dalpe, G., Leclerc, N., Vallee, A., Messer, A., Mathieu, M., De Repentigny, Y., and Kothary, R. (1998) *Mol. Cell. Neurosci.* **10,** 243–257
42. Helfand, B. T., Loomis, P., Yoon, M., and Goldman, R. D. (2003) *J. Cell Sci.* **116,** 2345–2359
43. Grasberger, H., De Deken, X., Miot, F., Pohlenz, J., and Refetoff, S. (2007) *Mol. Endocrinol.* **21,** 1408–1421
44. Bedard, K., and Krause, K. H. (2007) *Physiol. Rev.* **87,** 245–313
45. Suzukawa, K., Miura, K., Mitsushita, J., Resau, J., Hirose, K., Crystal, R., and Kamata, T. (2000) *J. Biol. Chem.* **275,** 13175–13178
46. Katoh, S., Mitsui, Y., Kitani, K., and Suzuki, T. (1997) *Biochem. Biophys. Res. Commun.* **241,** 347–351
47. Kamata, H., Tanaka, C., Yagisawa, H., and Hirata, H. (1996) *Neurosci. Lett.* **212,** 179–182
48. Goldsmith, W. (2001) *Crit. Rev. Biomed. Eng.* **29,** 441–600
49. Knapp, L. T., and Klann, E. (2002) *J. Neurosci. Res.* **70,** 1–7
50. Munnamalai, V., and Suter, D. M. (2009) *J. Neurochem.* **108,** 644–661
51. Tsatmali, M., Walcott, E. C., Makarenkova, H., and Crossin, K. L. (2006) *Mol. Cell. Neurosci.* **33,** 345–357
52. Sauer, H., Rahimi, G., Hescheler, J., and Wartenberg, M. (2000) *FEBS Lett.* **476,** 218–223
53. Tsatmali, M., Walcott, E. C., and Crossin, K. L. (2005) *Brain Res.* **1040,** 137–150
54. Wang, S., Rosengren, L. E., Hamberger, A., and Haglid, K. G. (1998) *Neuroreport* **9,** 3207–3211
55. Verdi, J. M., Schmandt, R., Bashirullah, A., Jacob, S., Salvino, R., Craig, C. G., Program, A. E., Lipshitz, H. D., and McGlade, C. J. (1996) *Curr. Biol.* **6,** 1134–1145
56. Zilian, O., Saner, C., Hagedorn, L., Lee, H. Y., Säuberli, E., Suter, U., Sommer, L., and Aguet, M. (2001) *Curr. Biol.* **11,** 494–501
57. Brewster, R., and Bodmer, R. (1995) *Development* **121,** 2923–2936
58. Spana, E. P., and Doe, C. Q. (1996) *Neuron* **17,** 21–26
59. Yu, W., Ling, C., and Baas, P. W. (2001) *J. Neurocytol.* **30,** 861–875
60. Dehmelt, L., Smart, F. M., Ozer, R. S., and Halpain, S. (2003) *J. Neurosci.* **23,** 9479–9490
61. Birbach, A. (2008) *BioEssays* **30,** 994–1002
62. Cochard, P., and Paulin, D. (1984) *J. Neurosci.* **4,** 2080–2094
63. Aletta, J. M., Angeletti, R., Liem, R. K., Purcell, C., Shelanski, M. L., and Greene, L. A. (1988) *J. Neurochem.* **51,** 1317–1320
64. Prather, R. S., Sims, M. M., Maul, G. G., First, N. L., and Schatten, G. (1989) *Biol. Reprod.* **41,** 123–132
65. Markiewicz, E., Ledran, M., and Hutchison, C. J. (2005) *J. Cell Sci.* **118,** 409–420
66. Mattia, E., Hoff, W. D., den Blaauwen, J., Meijne, A. M., Stuurman, N., and van Renswoude, J. (1992) *Exp. Cell Res.* **203,** 449–455
67. Lin, F., and Worman, H. J. (1993) *J. Biol. Chem.* **268,** 16321–16326

Developmental Biology:

Mammalian Numb-interacting Protein 1/Dual Oxidase Maturation Factor 1 Directs Neuronal Fate in Stem Cells

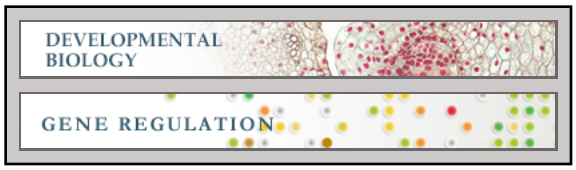

Karen A. M. Kennedy, Elena A. Ostrakhovitch, Shelley D. E. Sandiford, Thamara Dayarathna, Xiaojun Xie, Elaine Y. L. Waese, Wing Y. Chang, Qingping Feng, Ilona S. Skerjanc, William L. Stanford and Shawn S. C. Li

J. Biol. Chem. 2010, 285:17974-17985.
doi: 10.1074/jbc.M109.084616 originally published online March 16, 2010
